

See discussions, stats, and author profiles for this publication at: <https://www.researchgate.net/publication/27269972>

Deformation Properties of Nonadhesive Polyelectrolyte Microcapsules Studied with the Atomic Force Microscope

ARTICLE *in* THE JOURNAL OF PHYSICAL CHEMISTRY B · MARCH 2003

Impact Factor: 3.3 · DOI: 10.1021/jp026927y · Source: OAI

CITATIONS

93

READS

38

4 AUTHORS, INCLUDING:



Gleb Sukhorukov

Queen Mary, University of London

318 PUBLICATIONS **19,362** CITATIONS

SEE PROFILE



Olga I Vinogradova

Russian Academy of Sciences

111 PUBLICATIONS **3,381** CITATIONS

SEE PROFILE

Deformation Properties of Nonadhesive Polyelectrolyte Microcapsules Studied with the Atomic Force Microscope

V. V. Lulevich, I. L. Radtchenko, G. B. Sukhorukov, and O. I. Vinogradova*

Max Planck Institute for Polymer Research, Postfach 3148, 55021, Mainz, Germany, Laboratory of Physical Chemistry of Modified Surfaces, Institute of Physical Chemistry, Russian Academy of Sciences, 31 Leninsky Prospect, 117915 Moscow, Russia, and Max Planck Institute for Colloid and Interface Research, 14424 Golm, Potsdam, Germany

Received: September 6, 2002; In Final Form: November 7, 2002

We study the deformation of nonadhesive polyelectrolyte microcapsules under applied load using an atomic force microscope (AFM)-related force measuring device. Both “hollow” (water inside) and “filled” (water-polyanion solution inside) microcapsules are explored. The “filled” capsules were found to be much stiffer than “hollow” ones. The load–deformation profiles always included two regimes, characterized by different behavior. In the first regime, with a low applied load, capsule deformation is elastic and reversible. Above a certain load, capsules deform substantially and partly irreversibly. In this regime, the “hollow” capsules show variability in the reversibility, as well as in load–deformation profiles, which include different sectors (from substantial deformation at quasiconstant load to noisy regions). The “filled” capsules do not reveal such variability and become stiffer when the load is increased. After substantial deformation the “hollow” capsules enter a third region, in which major damage is caused by higher load. We show that the dramatic changes of the capsule’s mechanical properties after filling with polyelectrolyte reflect a combined effect of excess osmotic pressure inside them, changes in the shell stiffness, and possibly a formation inside capsules of an electrostatically stabilized 3D net structure.

Introduction

Polyelectrolyte multilayer capsules have been recently introduced as a novel type of nanoengineered microstructures.^{1,2} These capsules are made by layer-by-layer (LbL) adsorption³ of oppositely charged polyelectrolytes on surfaces of colloidal particles⁴ with subsequent removal of the template core. Microcapsules can be produced from a variety of materials as shell components, such as polyelectrolytes, proteins, nucleic acids, inorganic nanoparticles, dyes, and lipids. Shell properties such as thickness and permeability for certain classes of molecules can be tuned to match desired characteristics. These capsules can be filled with a wide class of molecules (for a review see ref 5). A relatively easy way to prepare them and to control their various properties suggests that they may be important in many areas, such as catalysis, agriculture, biotechnology, medicine, and more.

The mechanical and adhesion properties of the capsules have never been systematically studied (except as in ref 6), although knowledge of the deformation behavior of such a system is of both academic and industrial interest. Studying them is very important to evaluate their suitability for use, for instance, in development of drug delivery systems for injection in blood vessels. This can also help to understand the principle underlying the mechanical behavior of living cells.

This paper deals with deformation properties of nonadhesive polyelectrolyte microcapsules under applied load investigated with an AFM-related device. Forces between surfaces have been intensively studied with an AFM⁷ in so-called colloid probe mode.⁸ Electrostatic,⁸ steric,⁹ hydrophobic,^{10,11} capillary,¹²

hydrodynamic¹³ interactions, and more, have been measured. These studies have mainly focused on nondeformable surfaces, but in recent times the attention has shifted to AFM studies on deformable systems. Colloid studies on soft latex particles,^{12,14} bubbles,^{15–17} oil drops,¹⁸ and ice^{19,20} have been reported. We believe our work extends the area of applicability of the AFM technique for studying the deformation of new soft colloidal objects. Our aim here is to compare the mechanical properties of capsules filled with water and polyelectrolyte solution. The difference observed between these two types of capsules seem to be quite dramatic and suggests a possible connection between osmotic pressure, elasticity of the shell, and mechanical behavior of the capsules in contact with solids.

Materials and Methods

Materials. Sodium poly(styrene sulfonate) (PSS, Mw ~ 70 000 for shell walls and 1 000 000 for encapsulation, and poly-(allylamine hydrochloride) (PAH, Mw ~ 50 000) were obtained from Aldrich. Rhodamine 6G and ethylenediaminetetraacetic acid (EDTA) were purchased from Sigma. Y(NO₃)₃ was purchased from Merck. All commercial polyelectrolytes were used without further purification.

Dispersions of monodispersed weakly cross-linked melamine formaldehyde particles (MF-particles) with a diameter of $5.6 \pm 0.2 \mu\text{m}$ were purchased from Microparticles GmbH (Berlin, Germany).

Thin glass slides (0.17 mm) with optical quality surfaces were obtained from World Precision Instruments (Victoria, Australia). Glass spheres (radius $20 \pm 1 \mu\text{m}$) were purchased from Duke Sci. Co., CA. Imaging of glass slides and spheres with a regular AFM tip revealed the root-mean-square roughness over a 0.5

* To whom correspondence should be addressed. E-mail: vinograd@mpip-mainz.mpg.de.

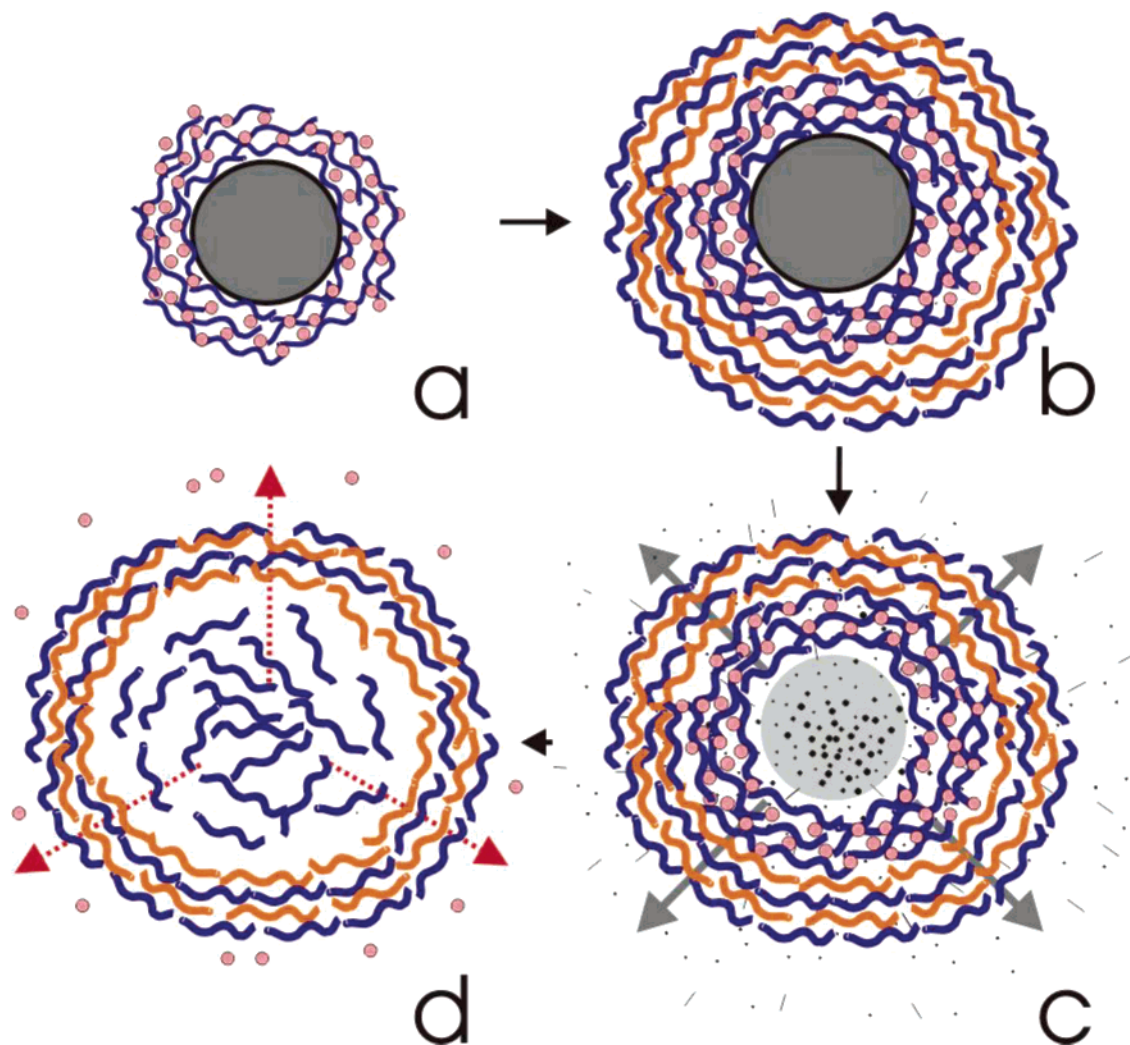


Figure 1. Scheme illustrating the preparation of the “filled” microcapsules.

$\pm 0.5 \mu\text{m}$ is in the range 3–4 nm, and the maximum peak-to-valley difference is less than 20 nm. Glass surfaces were cleaned by ethanol and plasma treatment.

Experiments were carried out in water and NaCl (99.99%, Aldrich) aqueous solutions with concentrations in the range from 1 mM to 1 M. In the case of NaCl solutions capsules were exposed to electrolytes for 7 days before the measurements. Water for solutions was prepared using a commercial Milli-Q system containing ion-exchange and charcoal stages.

Capsule Preparation. The capsules used in the work were of two types. Capsules of the first type are so-called “hollow” capsules, produced by LbL assembly of four pairs of polystyrene sulfonate (PSS) and polyallylamine (PAH) layers on melamine formaldehyde (MF) particles. MF-particles coated with PSS/PAH multilayers were dissolved in 3 M HCl and MF-oligomers were removed by washing, as described in ref 2. The second type is the so-called “filled” capsules, which contain polyelectrolyte (PSS) solution in the interior. The preparation of filled capsules comprises several steps (Figure 1). The first step (Figure 1a) consists of surface controlled precipitation of PSS on the surface of MF.²¹ Precipitation was achieved by complex formation with Y^{3+} ions in the presence of the colloidal templates, MF particles in our case. Mixing PSS with yttrium nitrate leads to insoluble complex formation $\text{PSS}^-/\text{Y}^{3+}$, which precipitates on any available surface. Actually, because MF particles offer much more surface than the walls of the vessels, almost all the PSS molecules are collected on them. For details

of this procedure see ref 22. Taking into account certain ratios between PSS molecules and the number of MF particles we are able to tune the density of PSS molecules precipitated on MF particles. In our experiments we have prepared samples with PSS surface density $12 \mu\text{g}/\text{cm}^2$ on the particle surfaces.

When PSS precipitation is completed the particles were treated for regular LbL assembly of four layer pairs PAH and PSS (Figure 1b). Core dissolution leads to formation of “double shell” structured capsules (Figure 1c). The inner shell formed by the PSS/Y^{3+} complex is not stable and can be decomposed either by metal-ion complex agents such as EDTA or in salt solution. Yttrium ions are readily expelled out of the outer stable shell formed by PSS/PAH, while PSS molecules are released into the capsule interior (Figure 1d).

In both cases of “hollow” and “filled” capsules the outer layer (i.e., in contact with the exterior solution) of the polyelectrolyte shell was formed by polyanions.

Atomic Force and Optical Microscopy. Load (force) vs deformation curves were measured with the Molecular Force Probe (MFP) 2D AFM (Asylum Co, Santa Barbara, CA). The MFP is equipped with a nanopositioning sensor that allows the controller to maintain unprecedented control over position when operating in a closed loop. This sensor can correct piezoceramic hysteresis and creep. The MFP was used in combination with an inverted optical microscope Olympus IX70 with a high-resolution immersion oil objective (100 \times), especially adjusted for the MFP 2D. This allowed simultaneous optical measure-

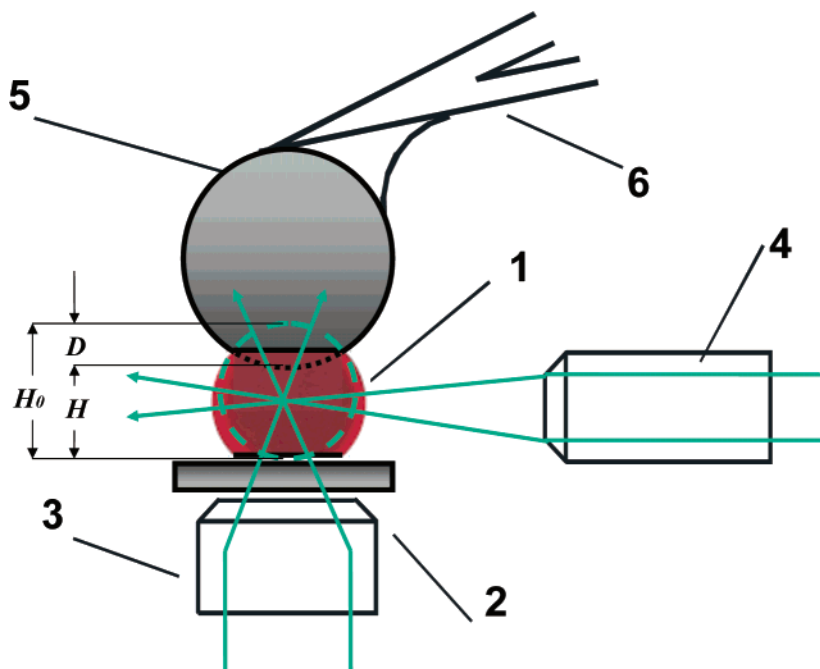


Figure 2. Schematic of the AFM force experiment. Dashed circle represents the undeformed capsule shape with the AFM diameter H_0 (the sphere–substrate distance without deformation). The absolute deformation $D = H_0 - H$, where H is the sphere–substrate distance with deformation, is used to calculate the relative deformation $\epsilon = D/H_0$.

ments, including the location of cantilever and capsules, and the capsule's shape.

We used V-shaped “stiff” cantilevers (Micromash, Estonia, 100 and 50 μm long, spring constants $k = 4$ and 40 N/m) and “soft” single beam cantilevers (Digital Instruments, 300 μm long, spring constant 0.05 N/m). Prior to mounting the colloid probe the spring constant of “soft” cantilevers was determined by measuring thermal noise power spectra²³ (“soft” cantilevers), included in the MFP software package. The constant of “stiff” cantilevers was determined by a resonance frequency calibration plot (Cantilevers catalog, Micromash, Estonia). Glass spheres were glued onto the apex of cantilevers with epoxy glue (UHU Plus, Germany).

As a confocal laser scanning microscope we used a commercial setup Leica TCS SP (Germany) equipped with a 100 \times oil immersion objective. The excitation wavelength was chosen according to the label rhodamine (525 nm). The confocal measurements were used to determine the 3D shape of the objects by z-position scanning with steps of 0.4 μm . They were also used to measure the concentration of polyelectrolyte inside the capsules via the fluorescence intensity coming from the interior of the rhodamine-labeled PSS-containing capsules. In this case we assumed that fluorescence is directly proportional to polymer concentration and used a calibration curve of fluorescence intensity of labeled PSS solution against polymer concentration.

Schematic of Experiment. A schematic of the AFM experiment is presented in Figure 2. A drop (50–100 μL) of water suspension of polyelectrolyte microcapsules (1) was deposited onto a thin glass substrate (2) fixed over the oil immersion objective of the inverted optical microscope (3). The capsule shell is very thin (about 20 nm). So, for capsule visualization we used back focused light (4), which can produce good shadows. To create contrast of solution we used the fluorescent dye CY-5. The optical image was recorded by an Olympus E-20P camera. The colloidal sphere (5) attached to a cantilever (6) was centered above the apex of a capsule located with a microscope with an accuracy of roughly 0.5 μm . The MFP was

then operated in force mode, measurements were performed at a speed of 2 $\mu\text{m/s}$. We have chosen such a speed to avoid any contribution to cantilever deflection caused by hydrodynamic drag on the sphere and/or cantilever.²⁴ Measurements performed at lower speed have not revealed any speed dependence of the force curves. Maximum loading force was up to 20 μN . To quantify the force data, the MFP photodiode was calibrated from the “constant compliance” region of force curves between the glass probe and the glass substrate in a region free from immobilized polyelectrolyte capsules.

Calculation of the Deformation Curve. The result of measurements represents the deflection Δ vs position of the piezo translator at single approach (loading)/retraction (unloading). The force F acting between the glass sphere and polyelectrolyte microcapsule was determined from the cantilever deflection $F = k\Delta$. The main difficulty with the AFM measurements on deformable systems is that there is normally no sharp transition between contact and noncontact due to the extended range of surface forces. In this study we simply assume that the zero of separation is at the point of the first measurable force.¹⁸ Then the deformation can be calculated as the difference between the position of the piezotranslator and cantilever deflection. The height of the capsule (AFM diameter) was determined as a difference between the position of the apex and the substrate, and was used as an independent way to determine the capsule diameter. The relative deformation ϵ of the capsule was then defined as a ratio of deformation to its height (or AFM diameter) as shown in Figure 2.

Results and Discussion

Adhesion. Both types of capsule are characterized by the absence of any adhesion to glass surfaces. We were unable to detect a pull-off force even with 0.05 N/m cantilevers. It was also seen with the optical microscope that capsules do not attach to the surface and can easily be removed with convection flow. The absence of adhesion is probably connected with the negative charge of both glass and capsule surfaces. Therefore, there is

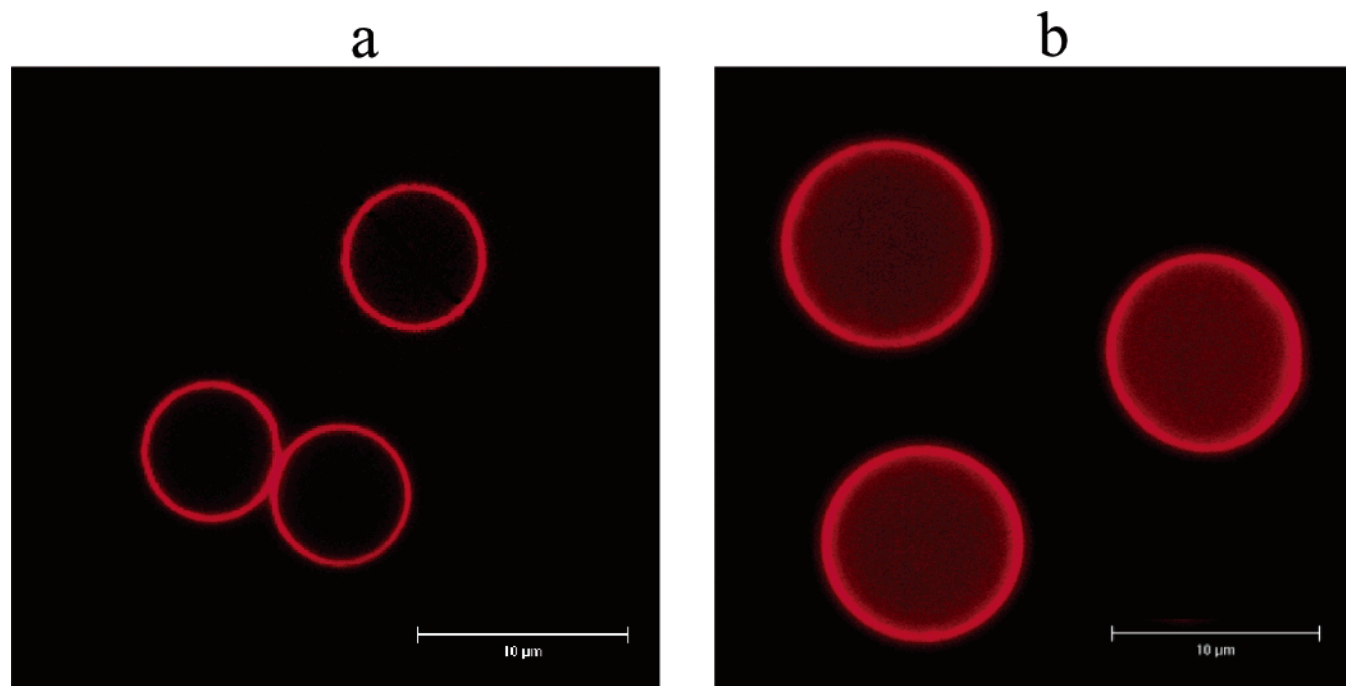


Figure 3. Typical confocal microscopy images of “hollow” (a) and “filled” (b) capsules.

electrostatic and steric repulsion between them, while the van der Waals force between a capsule and the surface across water is very weak.

“Hollow” Capsules. Confocal images of “hollow” capsules are shown in Figure 3a. The 3D scanning suggested that the “hollow” capsules are of spherical form and of the size of the original colloidal template.

We have performed several series of experiments, each included the measurements of about 20 capsules. Therefore, the so-called typical results we report below represent a generalization of many observations. Several percent of the capsules (typically 5% or less) have a tendency to be broken by the core dissolution process. In this case we have not observed the typical force curves (quantitatively), and these data were ignored in our analysis.

Typical load–deformation profiles for “hollow” capsules, compressed between a glass sphere and a plane in water are shown in Figure 4 (curves 1–3). The AFM diameter used to calculate ϵ was found to be equal to an optical (confocal) one. The “hollow” capsules are characterized by variability in their behavior. Despite that, one can detect some peculiarities in their deformation profiles, which always included three regimes.

In the *first regime* with low applied load (ϵ up to ~ 0.2 – 0.3 , inset in Figure 4), the capsule deformation is elastic and quasireversible. This suggests that in this regime the polyelectrolyte shell is elastic. There is some loading/unloading hysteresis, which is probably connected with the drainage of water in and out of the capsule. The hysteresis is, however, very weak, because the diffusion of water molecules through a shell is too slow compared with the time scale of the AFM force experiment.

The *second regime* ($\epsilon \sim 0.3$ – 0.8) is characterized by high nonlinearity in the load–deformation profile and only partial reversibility. The reversibility does not reveal any explicit dependence on the value of deformation and varies from one experiment to another. The load–deformation profile includes different sectors (from substantial deformation at the constant load to noisy regions in the data). Another important feature of this regime is a much higher hysteresis. These observations

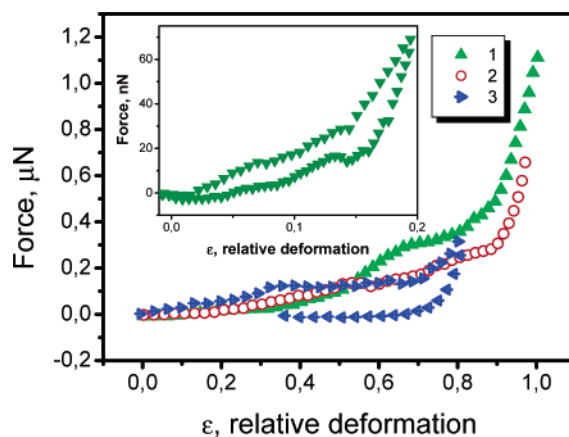


Figure 4. Typical load–deformation curves for “hollow” capsules. Curves 1 and 2 illustrate the loading until total destruction of the capsules. Curve 3 shows the loading (upper branch)/unloading (lower branch) cycle for a capsule deformed within the second regime. The inset shows the loading (upper branch)/unloading (lower branch) cycle for a capsule deformed within the first regime.

suggest that at higher load, typical for this regime, the deformation of the shell could become plastic. Beside that, water likely starts to drain faster from the capsule interior. It is likely that we deal with not just diffusion of water through the shell, but also its faster drainage due to some local ruptures of the shell.

After substantial deformation the capsules enter the *third region* ($\epsilon \sim 0.7$ – 0.9), in which major damage is caused by higher load. This region is characterized by an abrupt break in the load–deformation curve and practically zero reversibility. After loading, the optical image of the capsule disappears, which suggests its total destruction.

“Filled” Capsules. Confocal images of capsules filled with PSS are shown in Figure 3b. The “filled” capsules are significantly swollen and their confocal diameter is $9.0 \pm 0.5 \mu\text{m}$. Here, we also have not found any deviations of the capsule shape from the spherical one within the accuracy of the confocal 3D scanning.

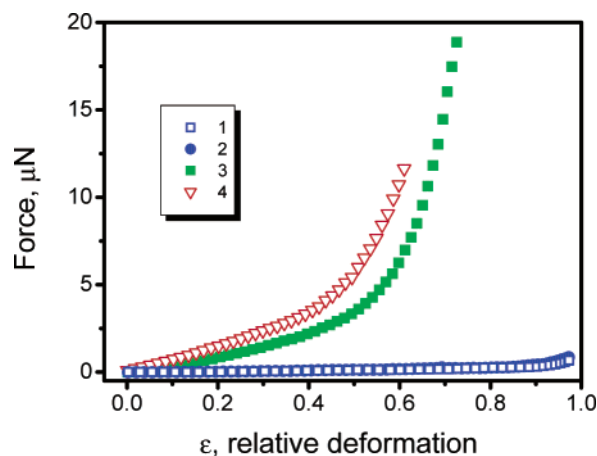


Figure 5. Typical load–deformation curves for “filled” capsules (curves 3 and 4). Curves 1 and 2 correspond to the case of “hollow” capsules and are given for comparison.

The load–deformation curves for “filled” capsules in water are given in Figure 5 (about 95% of the measured nearly 200 deformation profiles are confined between curves 3 and 4). Again, the capsule height measured with the AFM was found to be equal to the confocal diameter. Typical load–deformation profiles for “hollow” capsules immersed in water (curves 1 and 2) are included for comparison. It is seen that the “filled” capsules are much stiffer than “hollow”, i.e., they are deformed at 50–100 times higher load.

The “filled” capsules have two typical sectors in the load–deformation curve. As for “hollow” capsules the *first regime* (ϵ up to 0.1–0.15) is characterized by low hysteresis and reversibility of deformation. Further deformation (ϵ up to 0.5–0.8) corresponds to the *second regime* and shows an increase in hysteresis and irreversibility with applied load. Even for highly deformed capsules we never observed either their rupture, or disappearance of the optical image. Of course, the last observation is valid only within the range the applied load we used. We cannot exclude the possibility of capsule break-off at higher applied load. However, a higher load experiment would require the use of stiffer cantilevers and a modification of the existing setup. Therefore, filling the capsules with polyelectrolyte dramatically changes their mechanical properties.

The possible reason for increase in the stiffness of the “filled” capsules could be connected with excess osmotic pressure inside them, which in particular led to their swelling. The concentration of counterions is less or equal to the resulting PSS monomer concentration in the capsules. This was determined by confocal measurements as described above, and by an independent method via quenching of the rhodamine fluorescence. Both methods suggested that the concentration of counterions in the inner polyelectrolyte solution is ~ 0.1 M or less, so that the outer 1 M NaCl and even less concentrated solution could dramatically decrease the counterions osmotic pressure. To explore the dependence on osmotic pressure of counterions, we studied the deformation behavior of “filled” capsules in electrolyte solutions.

Typical load–deformation curves for different salt concentrations are given in Figure 6. These curves were obtained by averaging of the results of several series of experiments (from 3 to 5 capsules in each). One can see an expected tendency to increase deformation at the same load with electrolyte concentration. However, even at 1M, the load–deformation curve is well above the profile obtained for “hollow” capsules. The confocal microscope measurements show the reduction in diameter of capsules immersed in 1M solution, but only down

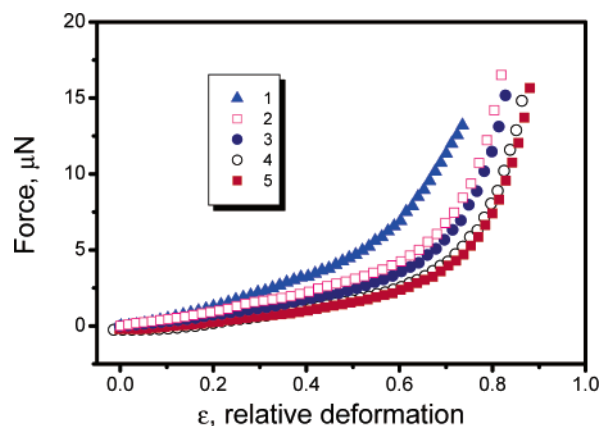


Figure 6. Typical load–deformation curves for “filled” capsules. Curve 1 corresponds to the case of a pure water, the curves from 2 to 5 are the results obtained for capsules immersed into 10^{-3} , 10^{-2} , 10^{-1} and 1 M NaCl solutions, correspondingly.

to $8.4 \pm 0.5 \mu\text{m}$ (The possible reduction in the capsule size in weaker electrolyte solutions is within the error of optical measurements). This confirms that there is some role for osmotic pressure in determining the stiffness of the capsules.

However, a single osmotic pressure mechanism cannot account for effect of electrolyte on the capsule mechanical properties. To explain the capsules stiffness in the concentrated electrolyte solutions, one can surmise that the elastic properties of the stretched shell of the swollen capsules could be changed irreversibly. The increase of the shell stiffness could be due to the stretching induced orientation of shell forming polymers, caused by the increase of the area of the shell as compared with “hollow” capsules. The shell stiffness is likely reduced with the added salt, which could be partly responsible for the deformation profiles on Figure 6, but does not return to the original state of the “hollow” capsule. One can also suggest the possibility of formation inside capsules of electrostatically stabilized 3D net formed by negatively charged molecules of PSS and positively charged traces of ions Y^{3+} (or MF fragments of the initial templates) as one factor of the increase of its stiffness. This, however, is beyond the scope of the present paper and will be discussed elsewhere.

Acknowledgment. Professor H. Möhwald is gratefully acknowledged for continuous support of this work and encouragement. We also thank A. A. Antipov, Dr. K. Mitsui, and Dr. G. E. Yakubov for assistance in organization of the experiment, and Professor R. G. Horn for helpful remarks on the manuscript. This work was supported in part by the Sofia Kovalevskaya Program funded by the Alexander von Humboldt Foundation and German Ministry of Education and Research.

References and Notes

- (1) Donath, E.; Sukhorukov, G. B.; Caruso, F.; Davis, S.; Möhwald, H. *Angew. Chem.* **1998**, *110*, 2323.
- (2) Sukhorukov, G. B.; Donath, E.; Davis, S.; Lichtenfeld, H.; Caruso, F.; Popov, V. I.; Möhwald, H. *Polym. Adv. Technol.* **1998**, *9*, 759.
- (3) Decher, G. *Science* **1997**, *277*, 1232.
- (4) Sukhorukov, G. B.; Donath, E.; Lichtenfeld, H.; Knippel, E.; Budde, A.; Möhwald, H. *Colloids Surf. A* **1998**, *137*, 253.
- (5) Sukhorukov, G. B. Designed Nano-Engineered Polymer Films on Colloidal Particles and Capsules. In *Novel Methods To Study Interfacial Layers*; Mobius, D., Miller, R., Eds.; Elsevier: 2001; p 384.
- (6) Gao, C.; Donath, E.; Moya, S.; Dudnik, V.; Möhwald, H. *Eur. Phys. J. E* **2001**, *5*, 21.
- (7) Binnig, G.; Quate, C. F.; Gerber, C. *Phys. Rev. Lett.* **1986**, *56*, 930.
- (8) Ducker, W. A.; Senden, T. J.; Pashley, R. M. *Nature* **1991**, *353*, 239.

- (9) Butt, H. J.; Kappl, M.; Mueller, H.; Raiteri, R. *Langmuir* **1999**, *15*, 2559.
- (10) Craig, V. S. J.; Ninham, B. W.; Pashley, R. M. *Langmuir* **1999**, *15*, 1562.
- (11) Yakubov, G. E.; Butt, H. J.; Vinogradova, O. I. *J. Phys. Chem. B* **2000**, *104*, 3407.
- (12) Vinogradova, O. I.; Yakubov, G. E.; Butt, H. J. *J. Chem. Phys.* **2001**, *114*, 8124.
- (13) Craig, V. S. J.; Neto, C.; Williams, D. R. M. *Phys. Rev. Lett.* **2001**, *87*, 054504.
- (14) Considine, R. F.; Hayes, R. A.; Horn, R. G. *Langmuir* **1999**, *15*, 1657.
- (15) Ducker, W. A.; Xu, Z.; Israelachvili, J. N. *Langmuir* **1994**, *10*, 3279.
- (16) Fielden, M. L.; Hayes, R. A.; Ralston, J. *Langmuir* **1996**, *12*, 3721.
- (17) Yakubov, G. E.; Vinogradova, O. I.; Butt, H. J. *J. Adhesion Sci. Technol.* **2000**, *14*, 1783.
- (18) Aston, D. E.; Berg, J. C. *J. Colloid Interface Sci.* **2001**, *12*, 461.
- (19) Butt, H. J.; Doeppenschmidt, A.; Huettl, G.; Mueller, E.; Vinogradova, O. I. *J. Chem. Phys.* **2000**, *113*, 1194.
- (20) Pittinger, B.; Fain, S. C.; Cochran, M. J.; Donev, J. M. K.; Robertson, B. E.; Szuchmacher, A.; Overney, R. M. *Phys. Rev. B* **2001**, *63*, 134102.
- (21) Dudnik, V.; Sukhorukov, G. B.; Radtchenko, I. L.; Möhwald, H. *Macromolecules* **2001**, *34*, 2329.
- (22) Radtchenko, I. L.; Sukhorukov, G. B.; Möhwald, H. *Colloids Surf. A* **2002**, *202*, 127.
- (23) Hutter, J. L.; Bechhoefer, J. *Rev. Sci. Instrum.* **1993**, *64*, 1868.
- (24) Vinogradova, O. I.; Butt, H. J.; Yakubov, G. E.; Feuillebois, F. *Rev. Sci. Instrum.* **2001**, *72*, 2330.